A&A 578, L5 (2015)
DOI: 10.1051/0004-6361/201526018

Astronomy & Astrophysics

Letter to the Editor

The elusive H I→H_2 transition in high-z damped Lyman-α systems

P. Noterdaeme[1], P. Petitjean[1], and R. Srianand[2]

[1] Institut d'Astrophysique de Paris, CNRS-UPMC, UMR 7095, 98bis bd Arago, 75014 Paris, France
e-mail: noterdaeme@iap.fr
[2] Inter-University Centre for Astronomy and Astrophysics, Post Bag 4, Ganeshkhind, 411 007 Pune, India

Received 4 March 2015 / Accepted 17 May 2015

ABSTRACT

We study the H_2 molecular content in high redshift damped Lyman-α systems (DLAs) as a function of the H I column density. We find a significant increase of the H_2 molecular content around $\log N(\mathrm{H\,I})$ ($\mathrm{cm^{-2}}$) ~ 21.5–22, a regime unprobed until now in intervening DLAs, beyond which the majority of systems have $\log N(H_2) > 17$. This is in contrast with lines of sight towards nearby stars, where such H_2 column densities are always detected as soon as $\log N(\mathrm{H\,I}) > 20.7$. This can qualitatively be explained by the lower average metallicity and possibly higher surrounding UV radiation in DLAs. However, unlike in the Milky Way, the overall molecular fractions remain modest, showing that even at a large N(H I) only a small fraction of overall H I is actually associated with the self-shielded H_2 gas. Damped Lyman-α systems with very high-N(H I) probably arise along quasar lines of sight passing closer to the centre of the host galaxy where the gas pressure is higher. We show that the colour changes induced on the background quasar by continuum (dust) and line absorption (H I Lyman and H_2 Lyman & Werner bands) in DLAs with $\log N(\mathrm{H\,I})$ ~ 22 and metallicity ~1/10 solar is significant, but not responsible for the long-discussed lack of such systems in optically selected samples. Instead, these systems are likely to be found towards intrinsically fainter quasars that dominate the quasar luminosity function. Colour biasing should in turn be severe at higher metallicities.

Key words. quasars: absorption lines – ISM: molecules

1. Introduction

The atomic to molecular hydrogen transition is a prerequisite process for star formation through the collapse of molecular clouds and therefore has important implications for the evolution of galaxies (e.g. Kennicutt & Evans 2012). The relative amount of dense molecular and diffuse atomic gas in nearby galaxies is found to be correlated with the hydrostatic pressure at the galactic mid-plane (Blitz & Rosolowsky 2006), which is driven by the gravity of gas and stars. This is a natural consequence of thermal equilibrium of the gas, leading to multiple phases under an external pressure (e.g. Wolfire et al. 1995). The transition between H I and H_2 can then be linked to a critical gas surface mass density above which star formation is triggered, inducing a Schmidt-Kennicutt relation (e.g. Schaye 2001; Altay et al. 2011; Lagos et al. 2011; Popping et al. 2014).

The local abundance of H_2 in the interstellar medium (ISM) depends on the balance between its formation, primarily on the surface of dust grains (e.g. Jura 1974; but also in the gas phase though the H^-+H→H_2+e^- reaction, Black et al. 1987), and its dissociation by UV photons. Because the dissociation occurs through Lyman and Werner band line transitions (e.g. Dalgarno & Stephens 1970), self-shielding becomes very efficient when H_2 absorption lines from several rotational levels become saturated (e.g. Draine & Bertoldi 1996). Dust grains also absorb Lyman and Werner band photons further contributing to decreasing the photo-dissociation rate. Theoretical microphysics models that include detailed treatment of the formation of H_2 onto dust grains and the dust- and self-shielding of H_2 show that the conversion from atomic to molecular occurs above a N(H I)-threshold that increases with decreasing metallicity (e.g. Krumholz et al. 2009; McKee & Krumholz 2010; Gnedin & Kravtsov 2011; Sternberg et al. 2014).

A sharp increase in the H_2 column densities has been first noticed above $\log N(\mathrm{H\,I})$ ~ 20.7 in the local Galactic ISM by Savage et al. (1977). In turn, the first studies of the Magellanic clouds by Tumlinson et al. (2002) did not reveal any dependence of the H_2 content on the H I column density. This was explained by a high average UV radiation due to intense local star formation activity together with lower metallicities. At high redshift, H_2 is generally detected in about 10% of damped Lyman-α systems (DLAs) or less (Petitjean et al. 2000; Ledoux et al. 2003; Noterdaeme et al. 2008). Physical conditions in these sub-solar metallicity systems indicate densities of the order of n ~ 50 $\mathrm{cm^{-3}}$ in the cold neutral medium, and ambient radiation field a few times the Draine field (e.g. Srianand et al. 2005; Neeleman et al. 2015). Noterdaeme et al. (2008) noted that the presence of H_2 does not strongly depend on the total neutral hydrogen column density up to $\log N(\mathrm{H\,I})$ ~ 21.5. They concluded that large molecular hydrogen content, as predicted by Schaye (2001) may be found at higher column densities.

Here, we investigate the H_2 content of high redshift H I-selected DLAs at the extreme H I column density end, a regime almost unprobed until now and only made reachable very recently thanks to very large DLA datasets (Noterdaeme et al. 2012) and high-resolution spectroscopic follow-up.

2. The atomic to molecular hydrogen transition

We have recently searched for H_2 in four extremely strong DLAs (ESDLAs, defined as $\log N(\mathrm{H\,I}) \geq 21.7$, Noterdaeme et al. 2014) using the Ultraviolet and Visual Echelle Spectrograph (UVES) on the Very Large Telescope (VLT). This brings the number of ESDLAs with H_2 searches (all with VLT/UVES) to seven. Details of H I and H_2 measurements in these ESDLAs are summarised in Table 1. Combining this with other measurements we explore the H_2 content as a function of N(H I) in DLAs while refraining from drawing any conclusion on the overall H_2 detection rate. We can do so since the DLAs used for this study were selected only on the basis of their neutral hydrogen content.

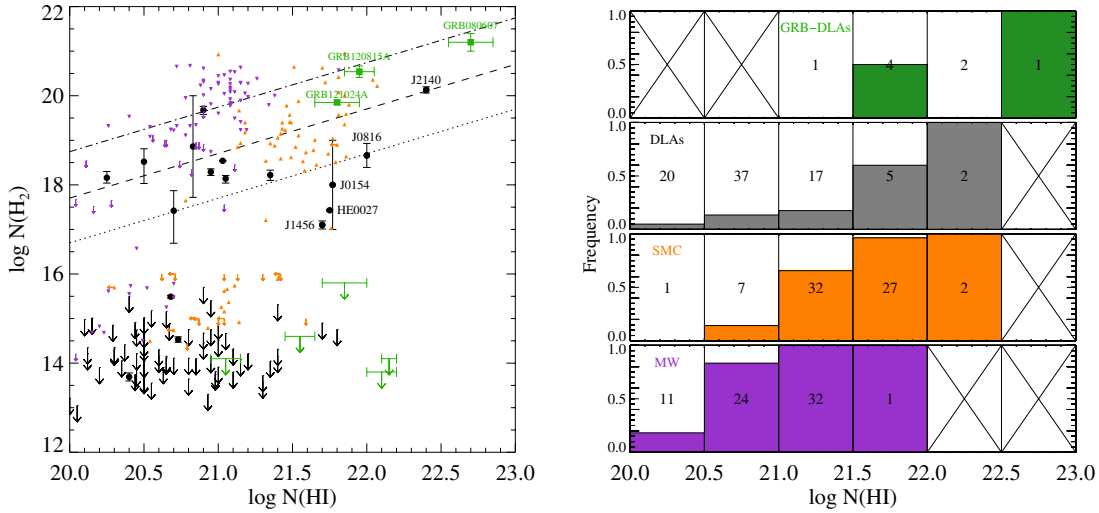

Fig. 1. *Left*: column density of H_2 as a function of that of H I. Data for high-redshift ($z > 1.8$) quasar-DLAs (black points and arrows) are from Noterdaeme et al. (2008; updated to more recent determination in a few cases, Ivanchik et al. 2010; Rahmani et al. 2013; Albornoz Vásquez et al. 2014). Additional measurements in ESDLAs are from Noterdaeme et al. (2015) and Guimarães et al. (2012). Data for GRB-DLAs (green) are from Ledoux et al. (2009, upper limits), Prochaska et al. (2009, GRB 080607), Krühler et al. (2013, GRB 120815A), and Friis et al. (2015, GRB 121024A). With the exception of GRB 080607 and GRB 121024A, in which damped H_2 lines allow for accurate column density measurement at medium spectral resolution, all high-z values (quasar and GRB DLAs) are from UVES data. Purple (resp. orange) points represent measurements in the Milky Way (resp. SMC). The dotted, dashed, and dash-dotted lines represent average molecular fractions of, respectively, $f = 0.1$, 1, and 10%. *Right*: frequency of H_2 detection as a function of the H I column density. For each N(H I) bin, systems with $\log N(H_2) \geq 17$ are coded in colour, and systems with $\log N(H_2) < 17$ are shown in white. Systems with upper limits that are not stringent (i.e. above $\log N(H_2) = 17$) are not taken into account. The numbers in each box indicate the total number of systems contributing to the bin. Crossed boxes have no statistics.

Table 1. H_2 in ESDLAs with $\log N(\mathrm{H\,I}) \geq 21.7$.

Quasar	z_{abs}	$\log N$(H I)	$\log N(H_2)$	Ref.
HE 0027−1836	2.402	21.75 ± 0.10	17.43 ± 0.02	1
Q J0154+1935	2.251	21.75 ± 0.15	~18	2
Q 0458−0203	2.040	21.70 ± 0.10	≤14.60	3
Q J0816+1446	3.287	22.00 ± 0.10	18.66 ± 0.30	4
Q 1157+0128	1.944	21.80 ± 0.10	≤14.50	1
Q J1456+1609	3.352	21.70 ± 0.10	17.10 ± 0.09	2
Q J2140−0321	2.340	22.40 ± 0.10	20.13 ± 0.07	2

References. (1) Rahmani et al. (2013); (2) Noterdaeme et al. (2015); (3) Noterdaeme et al. (2008); (4) Guimarães et al. (2012).

For this reason, we do not include recent H_2 detections obtained by directly targeting systems based on the presence of cold gas[1].

In the left panel of Fig. 1, we compare the total H_2 column density versus that of H I in our extended high-z DLA sample (Noterdaeme et al. 2008 and the new ESDLAs) with values in the local Galactic ISM (Savage et al. 1977), in the Small Magellanic Cloud (SMC; Welty et al. 2012), and in DLAs associated with γ-ray burst afterglows (GRB-DLAs). In the overall population, we clearly see a bimodality in the distribution of $N(H_2)$: most detections have $\log N(H_2) > 17$, far above the typical detection limits (a few times 10^{14} cm^{-2}). In the following, we denote as "strong" (resp. "weak") the systems with $\log N(H_2) > 17$ (resp. <17). The right panel shows the distribution of systems in each of these populations as a function of the H I column density[2]. We find that H_2 is detected with column densities higher than 10^{17} cm^{-2} in four (five if we include the possible H_2 detection in the DLA towards J0154+1935) ESDLAs out of seven. This is significantly higher than the value seen in the the overall DLA population (~10%, Noterdaeme et al. 2008; Balashev et al. 2014 or possibly less, Jorgenson et al. 2014). The increase in the fraction of strong H_2 systems is significant but not as sharp as is seen in the Milky Way or in the Small Magellanic Cloud. In addition, the overall molecular fractions remain modest (~1% or less).

To explain this, it must be noted that the multi-phase nature of the neutral gas is not equivalently probed by the different samples. The values corresponding to the Milky Way come from lines of sight towards nearby stars that are located only within ~100 pc. These should therefore probe a single cloud that produces most of the total observed column density and in which the N(H I) and $N(H_2)$ can be directly related by microphysics. The situation is already different towards stars in the Magellanic clouds for which the observed column densities may include gas from different clouds or phases along the same line of sight. Welty et al. (2012) also argued that previous N(H I) determinations in the SMC were overestimated because they were derived from 21 cm emission, which averages structures in the ISM at scales smaller than the radio beams. Indeed, once the N(H I)-values are more accurately determined using Ly-α-absorption (i.e. along the same pencil-beam line of sight as used for H_2 measurements) higher molecular fractions are found in the SMC, revealing a clearer segregation between the strong and weak H_2 populations around $\log N(\mathrm{H\,I}) \sim 21$[3]. In DLAs, the H I and H_2 column densities are measured through UV absorption along the same line of sight. However, a single quasar sight line likely samples multiple gas components having

[1] Either because of the detection of C I absorption (Srianand et al. 2008; Noterdaeme et al. 2010), the presence of 21 cm absorption (Srianand et al. 2012), or direct evidence of H_2 lines (Balashev et al. 2014).

[2] For simplicity only the total H_2 column density is used for a given DLA. In spite of this, the total $N(H_2)$ is dominated in all cases by a few components that individually also have $\log N(H_2) > 17$.

[3] We caution that part of the background stars were targeted for stellar studies (hence generally probing low extinction lines of sight), while others were specifically targeted to study the properties of dust, providing highly reddened lines of sight.

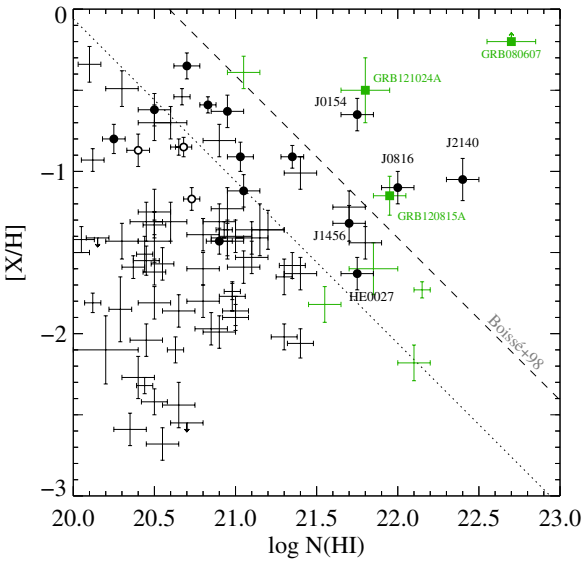

Fig. 2. Metallicity versus H I column density. Data samples and corresponding symbols are as in Fig. 2. Filled (resp. unfilled) circles represent systems in which H_2 has been detected with $\log N(H_2) \geq 17$ (resp. $\log N(H_2) < 17$). The dotted (resp. dashed) line represents a constant $\log N(\mathrm{Zn\,II}) = 12.5$ (resp. $\log N(\mathrm{Zn\,II}) = 13.15$).

different physical conditions, as seen from the excitation of different species (e.g. Srianand et al. 2005; Liszt 2015; Noterdaeme et al. 2015). In addition, at a given redshift, different DLAs probe different galaxies with their own sets of physical conditions, which may contribute to smoothing the observation of any underlying transition. Recently, Balashev et al. (2015) have used chlorine to show that the *local* metallicity and molecular fraction in the H_2 components could be much higher than the line-of-sight averaged value, although this does not tell us whether the remaining H I is located in outer layers or in unrelated interloping clouds.

Our results show that a large amount of H I in ESDLAs could indeed be unrelated to H_2. This is also supported by the similar H_2 column densities seen in several much lower N(H I) systems. The large N(H I) probably results from a low impact parameter of the line of sight relative to the galactic centre (Noterdaeme et al. 2014) where the covering factor of H_2-bearing gas would be higher owing to higher ISM pressure (Blitz & Rosolowsky 2006).

The situation could be similar along the lines of sight towards afterglows of long-duration γ ray bursts (GRBs) where DLAs are often seen with $\log N(\mathrm{H\,I}) > 22$ (e.g. Jakobsson et al. 2006). As these GRBs are linked to the death of a massive star (Bloom et al. 1999), they are probably related to star forming regions that are typically denser and closer to the centre of the host galaxy than quasar-DLAs (Pontzen et al. 2010). Because GRB-DLAs may be subject to a very intense UV radiation field (Tumlinson et al. 2007) one has to exercise caution when comparing them with quasar-DLAs. Nevertheless, although the sample is still small it appears that the detection rate is consistent with that seen in quasar-DLAs albeit with larger molecular fractions. This further supports the idea that most high column density lines of sight likely probe the central regions of a galaxy.

ESDLAs are very rare and huge surveys are needed to find them (Noterdaeme et al. 2009, 2012). However, one could question the fact that the H I to H_2 transition may induce a bias in the selection of the quasars against the detection of the corresponding systems.

3. The effect of ESDLAs on the colours of the background quasar

In Fig. 2, we identify the H_2-bearing DLAs in the N(H I)-metallicity plane. Interestingly three quasar-DLAs and four GRB-DLAs are now known beyond the limit for significant dust obscuration proposed by Boissé et al. (1998) and long discussed in the literature (e.g. Neeleman et al. 2013). Six of these DLAs show self-shielded H_2. As observed by Petitjean et al. (2006) and as predicted by some models (e.g. Krumholz et al. 2009; Sternberg et al. 2014), the H_2 detection rate is higher at high metallicity. However, the metallicity at which H_2 is found increases with decreasing N(H I). The presence of H_2 could be more closely related to the column density of dust grains (Noterdaeme et al. 2008): using the column density of undepleted elements as a first-order proxy for that of dust (Vladilo & Péroux 2005), we can see that 10 of the 15 systems above a line of constant $\log N(\mathrm{Zn\,II}) = 12.5$ have $\log N(H_2) \geq 17$, while this fraction is only 4/66 below.

Continuum absorption by dust and the absorption from lines in the Lyman series of H I and Lyman and Werner bands of H_2 can significantly affect the quasar transmitted flux in the different bands when column densities become very large. We quantify these effects by calculating the transmission for different H I and H_2 column densities and different reddening. For each absorption situation, the induced colour changes depend on the absorption redshift, the filter responses, and the input spectrum (quasar continuum plus Ly α forest). For simplicity, we fixed $z_{\rm abs} = 2.35$ (i.e. the redshift of our strongest ESDLA towards J2140−0321), used the filter responses of the Sloan Digital Sky Survey (SDSS, York et al. 2000), and considered a flat quasar spectrum. Our results are shown in Fig. 3. We empirically checked that assuming a flat spectrum has little effect on the results. To this end, we introduced fake absorbers with known properties (N(H I), $N(H_2)$, and dust) in real non-BAL quasar spectra (with emission redshift close to that of J2140−0321) and derived the colour changes. We find very good agreement (~0.01 mag for r, i, z and 0.05 mag in g) with our simple model[4].

In the case of J2140−0321, we find that the damped Ly α line alone severely affects the g-band (by 0.18 mag). Similarly, the strong H_2 absorption lines raise the u-band magnitude by ~0.26 mag. The importance of these line absorption is similar to that of the continuum absorption owing to the presence of dust (for $E(B-V) \sim 0.05$, estimated through SED profile fitting, see Noterdaeme et al. 2014) in these two bands. While the overall colour excesses estimated for J2140−0321 are likely not large enough to push the quasar out of typical colour-selections, it is still significant. We note that a DLA with the same characteristics as those of the DLA associated with GRB 080607 would in turn very likely escape current colour-based selections. In addition, even if such a spectrum were to be obtained, then the DLA would still be hard to recognise using automated detection procedures because of the little transmitted flux remaining between damped H I and H_2 absorption lines. This shows that alternative selection of quasars, based for example on NIR photometry (e.g. Fynbo et al. 2013; Krogager et al. 2015), are important in order to avoid biasing against intervening systems beyond the neutral to molecular transition. A promising technique for identifying these systems is to search for C I absorption (Ledoux et al. 2015).

[4] This consistency check is not possible in the u-band because the corresponding wavelength range is not covered by the SDSS spectra.

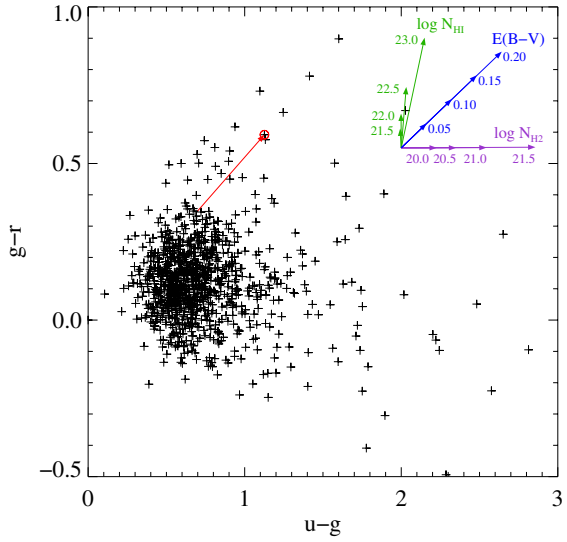

Fig. 3. Colours of J2140−0321 compared to those of other non-BAL quasars from SDSS-III at the same redshift. The arrows in the top right corner illustrate the estimates of colour excess due to H I, H_2, and dust (assuming SMC extinction law) at z_{abs} = 2.34. We note that because transmission is multiplicative, the corresponding magnitudes are additive and so are the colour vectors. The red arrow shows the estimated colour excess of J2140−0321 (circled red) due to the intervening ESDLA.For comparison, the colour excess that would produce a DLA with same column densities and reddening as those associated with GRB 080607 would reach the full ranges covered by both axes.

4. Conclusions

We have extended the study of H_2 in DLAs to the very high H I column density end, allowing us to uncover a significant increase in the fraction of strong H_2 systems (that we define as having $\log N(H_2) > 17$) at $\log N(\mathrm{H\,I}) > 21.5$. While the high N(H I)-threshold is qualitatively consistent with expectations from theoretical models describing H_2 microphysics, the mean molecular fraction in these systems remains relatively low. This can be explained by the quasar lines of sight having long path lengths through galaxies. In this picture, most of the H I is due to clouds unrelated to the molecular phase probed by H_2. The threshold for *local* H I to H_2 conversion in high-z DLAs could actually occur at N(H I) and metallicities similar to those in the Milky Way disc. The large H_2 column densities observed in EDLAs (with $\log N(\mathrm{H\,I}) > 21.7$) could simply be due to the line of sight passing closer to the galaxy centre as shown by Noterdaeme et al. (2014), where the ISM pressure is higher and so is the probability of intercepting a molecular cloud. This is also consistent with the skewed N(H I)-distributions observed in samples of absorbers selected for their high molecular content. The N(H I)-distribution of ~20 strong H_2 absorbers directly selected from the SDSS (Balashev et al. 2014) is indeed biased towards high N(H I) systems. Similarly, Ledoux et al. (2015) observe an excess of strong N(H I)-systems among C I-selected absorbers, which appear to harbour high molecular content. We note that high molecular content is also found in some low N(H I) absorbers (e.g. Srianand et al. 2008; Noterdaeme et al. 2010), which shows that the conversion from atomic to molecular hydrogen due to microphysics (which occurs on pc-scales, e.g. Srianand et al. 2013) does not require very high N(H I) (see also Muzahid et al. 2015).

We have investigated the impact on the quasar colours by the presence of systems beyond the neutral to molecular transition and showed that selection of quasars with NIR photometry would be important in order to avoid biasing against the detection of systems with high molecular content.

Acknowledgements. We thank the referee for careful reading of the manuscript and insightful remarks that helped improving the clarity of this paper.

References

Albornoz Vásquez, D., Rahmani, H., Noterdaeme, P., et al. 2014, A&A, 562, A88
Altay, G., Theuns, T., Schaye, J., Crighton, N. H. M., & Dalla Vecchia, C. 2011, ApJ, 737, L37
Balashev, S. A., Klimenko, V. V., Ivanchik, A. V., et al. 2014, MNRAS, 440, 225
Balashev, S. A., Noterdaeme, P., Klimenko, V. V., et al. 2015, A&A, 575, L8
Black, J. H., Chaffee, F. H., & Foltz, C. B. 1987, ApJ, 317, 442
Blitz, L., & Rosolowsky, E. 2006, ApJ, 650, 933
Bloom, J. S., Kulkarni, S. R., Djorgovski, S. G., et al. 1999, Nature, 401, 453
Boissé, P., Le Brun, V., Bergeron, J., & Deharveng, J.-M. 1998, A&A, 333, 841
Dalgarno, A., & Stephens, T. L. 1970, ApJ, 160, L107
Draine, B. T., & Bertoldi, F. 1996, ApJ, 468, 269
Friis, M., De Cia, A., Krühler, T., et al. 2015, MNRAS, accepted [arXiv:1409.6315]
Fynbo, J. P. U., Geier, S. J., Christensen, L., et al. 2013, MNRAS, 436, 361
Gnedin, N. Y., & Kravtsov, A. V. 2011, ApJ, 728, 88
Guimarães, R., Noterdaeme, P., Petitjean, P., et al. 2012, AJ, 143, 147
Ivanchik, A. V., Petitjean, P., Balashev, S. A., et al. 2010, MNRAS, 404, 1583
Jakobsson, P., Fynbo, J. P. U., Ledoux, C., et al. 2006, A&A, 460, L13
Jorgenson, R. A., Murphy, M. T., Thompson, R., & Carswell, R. F. 2014, MNRAS, 443, 2783
Jura, M. 1974, ApJ, 191, 375
Kennicutt, R. C., & Evans, N. J. 2012, ARA&A, 50, 531
Krogager, J.-K., Geier, S., Fynbo, J. P. U., et al. 2015, ApJS, 217, 5
Krühler, T., Ledoux, C., Fynbo, J. P. U., et al. 2013, A&A, 557, A18
Krumholz, M. R., Ellison, S. L., Prochaska, J. X., & Tumlinson, J. 2009, ApJ, 701, L12
Lagos, C. D. P., Baugh, C. M., Lacey, C. G., et al. 2011, MNRAS, 418, 1649
Ledoux, C., Petitjean, P., & Srianand, R. 2003, MNRAS, 346, 209
Ledoux, C., Vreeswijk, P. M., Smette, A., et al. 2009, A&A, 506, 661
Ledoux, C., Noterdaeme, P., Petitjean, P., & Srianand, R. 2015, A&A, in press, DOI: 10.1051/0004-6361/201524122
Liszt, H. S. 2015, ApJ, 799, 66
McKee, C. F., & Krumholz, M. R. 2010, ApJ, 709, 308
Muzahid, S., Srianand, R., & Charlton, J. 2015, MNRAS, 448, 2840
Neeleman, M., Wolfe, A. M., Prochaska, J. X., & Rafelski, M. 2013, ApJ, 769, 54
Neeleman, M., Prochaska, J. X., & Wolfe, A. M. 2015, ApJ, 800, 7
Noterdaeme, P., Ledoux, C., Petitjean, P., & Srianand, R. 2008, A&A, 481, 327
Noterdaeme, P., Petitjean, P., Ledoux, C., & Srianand, R. 2009, A&A, 505, 1087
Noterdaeme, P., Petitjean, P., Ledoux, C., et al. 2010, A&A, 523, A80
Noterdaeme, P., Petitjean, P., Carithers, W. C., et al. 2012, A&A, 547, L1
Noterdaeme, P., Petitjean, P., Pâris, I., et al. 2014, A&A, 566, A24
Noterdaeme, P., Srianand, R., Rahmani, H., et al. 2015, A&A, 577, A24
Petitjean, P., Srianand, R., & Ledoux, C. 2000, A&A, 364, L26
Petitjean, P., Ledoux, C., Noterdaeme, P., & Srianand, R. 2006, A&A, 456, L9
Pontzen, A., Deason, A., Governato, F., et al. 2010, MNRAS, 402, 1523
Popping, G., Somerville, R. S., & Trager, S. C. 2014, MNRAS, 442, 2398
Prochaska, J. X., Sheffer, Y., Perley, D. A., et al. 2009, ApJ, 691, L27
Rahmani, H., Wendt, M., Srianand, R., et al. 2013, MNRAS, 435, 861
Savage, B. D., Bohlin, R. C., Drake, J. F., & Budich, W. 1977, ApJ, 216, 291
Schaye, J. 2001, ApJ, 562, L95
Srianand, R., Petitjean, P., Ledoux, C., Ferland, G., & Shaw, G. 2005, MNRAS, 362, 549
Srianand, R., Noterdaeme, P., Ledoux, C., & Petitjean, P. 2008, A&A, 482, L39
Srianand, R., Gupta, N., Petitjean, P., et al. 2012, MNRAS, 421, 651
Srianand, R., Gupta, N., Rahmani, H., et al. 2013, MNRAS, 428, 2198
Sternberg, A., Le Petit, F., Roueff, E., & Le Bourlot, J. 2014, ApJ, 790, 10
Tumlinson, J., Prochaska, J. X., Chen, H.-W., Dessauges-Zavadsky, M., & Bloom, J. S. 2007, ApJ, 668, 667
Tumlinson, J., Shull, J. M., Rachford, B. L., et al. 2002, ApJ, 566, 857
Vladilo, G., & Péroux, C. 2005, A&A, 444, 461
Welty, D. E., Xue, R., & Wong, T. 2012, ApJ, 745, 173
Wolfire, M. G., Hollenbach, D., McKee, C. F., Tielens, A. G. G. M., & Bakes, E. L. O. 1995, ApJ, 443, 152
York, D. G., Adelman, J., Anderson, Jr., J. E., et al. 2000, AJ, 120, 1579